

Broadband multilayer-coated normal incidence blazed grating with $\sim 10\%$ diffraction efficiency through the 13–16 nm wavelength region

Lichao Zhang,^{1,*} Hui Lin,² Chunshui Jin,¹ Hongjun Zhou,³ and Tonglin Huo³

¹State Key Lab of Applied Optics, Changchun Institute of Optics, Fine Mechanics and Physics, Chinese Academy of Sciences, Changchun 130033, China

²State Key Laboratory of Precision Measurement Technology and Instruments, Department of Precision Instruments, Tsinghua University, Beijing 100084, China

³National Synchrotron Radiation Laboratory, University of Science and Technology of China, Hefei 230029, China

*Corresponding author: lichao@yahoo.com.cn

Received December 23, 2008; revised February 12, 2009; accepted February 13, 2009;
posted February 18, 2009 (Doc. ID 105696); published March 11, 2009

Diffraction gratings used in extreme UV are typically coated with periodic multilayer thin films. These coatings have a small bandwidth, thus leading to a narrow usable spectral region of multilayer gratings. Well-designed aperiodic multilayer coatings could provide high reflectivity over a much broader wavelength region, so they could broaden the usable spectral region of multilayer gratings. We designed and deposited an aperiodic Mo/Si multilayer coating onto a blazed grating substrate. At an incidence angle of 10° , the -2 nd-order diffraction efficiency of the multilayer grating is $\sim 10\%$ through the wavelength range of 13–16 nm.

© 2009 Optical Society of America

OCIS codes: 050.1950, 120.4610, 310.1620, 340.7480.

Diffraction grating is a key element of extreme UV (EUV) spectrometers that are widely used in astrophysics, plasma diagnostics, and so on. When the EUV grating is used at normal incidence, periodic multilayer interference coating composed of alternate layers of scattering material (absorber) and transmissive material (spacer) should be deposited on the grating substrate to enhance diffraction efficiency. In recent years, both multilayer laminar gratings and multilayer blazed gratings with high diffraction efficiencies have been fabricated [1–4]. Nevertheless, these multilayer gratings provide a narrow usable spectral region in which the diffraction efficiency is sufficiently high for the applications. This is due to the fact that the diffraction efficiency of a normal incidence multilayer grating is the product of two factors, the grating groove efficiency and the reflectivity of the multilayer coating [1,5]. On one hand, the grating groove efficiency is a weak function of wavelength; on the other hand, however, the wavelength bandwidth of periodic multilayer coating is narrow, for example, typically < 1 nm (FWHM) in the 13–16 nm wavelength region. So it restricts the applications of multilayer gratings in spectrometers that need a broad, usable region.

A simple method to achieve a broader usable spectral region for a multilayer grating is to deposit different periodic multilayer coatings onto different areas of one grating substrate. Each periodic multilayer coating operates on a specific narrow-wavelength region; thus a wider usable spectral region could be achieved. This method has been used to fabricate multilayer gratings for the Extreme Ultraviolet Spectrometer [6]. When this method is adopted, only a part of the grating is actually used for each wavelength region, thus leading to a lower photon flux for each wavelength region.

We develop another approach to get a broad usable spectral region for a multilayer grating by changing the structure of the multilayer coating. Aperiodic multilayer coatings have been developed to tailor spectral or angular reflectivity for both hard x-ray [7] and EUV [8] applications. By using appropriate aperiodic coating design, broadband reflectivity in a wide wavelength region could be realized [9]. Here we apply the broadband multilayer coating to broaden the usable spectral range of EUV multilayer gratings. By depositing a well-designed aperiodic Mo/Si multilayer onto a blazed grating substrate, we get $\sim 10\%$ diffraction efficiency through 13–16 nm wavelength region at an incident angle of 10° . In this Letter, we describe the design and fabrication process and present diffraction-efficiency-measurement results of the aperiodic multilayer grating.

We wrote a computation code to optimize the coating structure. This code is based on the genetic algorithm, which is an effective method to optimize aperiodic multilayer coatings shown by Aquila *et al.* [10]. By using optical constants of Mo and Si determined by Souffi and Gullikson [11,12], we got an optimized coating structure, as shown in Table 1. The calculated reflectivity of this aperiodic multilayer coating structure is illustrated in Fig. 1. The coating yields an average theoretical reflectivity of 22.53% in the region of 13–16 nm at an incident angle of 10° .

The coating was deposited onto a blazed grating substrate fabricated by using the method described in [13]. The grating was fabricated on a finely polished fused-silica substrate of $30\text{ mm} \times 30\text{ mm}$ in area and 1 mm in thickness. The groove density was 2400 lines/mm. To achieve high groove efficiency in the range of 13–16 nm in the -2 nd order at 10° incident angle, the blaze angle was designed as 2° , which corresponds to a blaze wavelength of 14.5 nm. We

Table 1. Multilayer Coating Structure^a

substrate/3.0H/9.1L/3.8H/3.3L/3.5H/9.3L/4.0H/3.6L/3.8H/3.5L/3.6H/3.1L/3.2H/2.9L/3.6H/3.6L/3.8H/3.7L/3.7H/3.7L/3.5H/3.5L/3.1H/3.1L/3.3H/3.6L/3.7H/3.9L/3.8H/4.0L/3.8H/4L/3.8H/4.1L/3.7H/4.1L/3.6H/4.3L/3.5H/5.3L/3.5H/6.3 L/air
--

^aIn the expression H and L denote 1-nm-thick Mo and Si, respectively.

used atomic force microscopy (AFM) to measure the actual grating profile and to deduce blaze and anti-blaze angles by using the algorithm introduced in [14]. Five locations in or around the sample center were measured; the average blaze and anti-blaze angles are 2.0° and 9.4° , respectively. The calculated groove efficiency of the grating substrate and the diffraction efficiency of the multilayer grating in the -2nd order are also shown in Fig. 1. Calculations were made by using a code based on the differential method of grating theory [15].

The coating process took place in an Oxford Ionfab ion-beam sputtering system. Layer thicknesses were controlled by a quartz crystal monitor. A fused-silica substrate without a grating pattern was also coated simultaneously with the grating to serve as the witness flat, which is used to measure the reflectivity of the aperiodic multilayer coating.

Reflectivity and diffraction efficiency measurements were made at the Spectral Radiation Standard and Metrology Beamline of the National Synchrotron Radiation Laboratory of China. The beamline is equipped with a scanning monochromator that uses a spherical grating with spectral resolution ($\lambda/\Delta\lambda$) of ~ 192 . To suppress the signal of higher harmonics, a silicon nitride filter was mounted after the monochromator. Samples were measured in a reflectometer, allowing the sample holder and the photodiode detector to move in several degrees of freedoms. The incident radiation was about 80% *s* polarization (electric vector parallel to the groove), and the spot size on the sample was $3\text{ mm} \times 1\text{ mm}$. When measuring the diffraction efficiency of the multilayer grating, a slit of $\sim 0.8\text{ mm}$ width was mounted in front of the detector to resolve diffraction orders.

We first calibrated the wavelength scale of the monochromator by measuring the Si *L* absorption

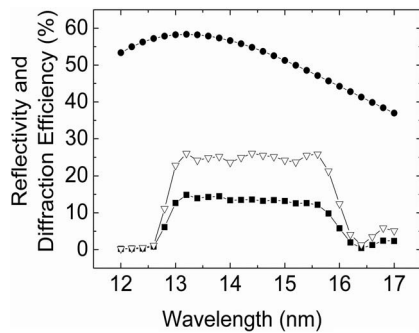


Fig. 1. Calculated reflectivity of multilayer coating (empty triangles) with the structure in Table 1, calculated groove efficiency of the grating substrate (filled circles) using blaze and anti-blaze angles deduced from AFM results, calculated -2nd -order diffraction efficiency of the aperiodic multilayer grating at an incidence angle of 10° (filled squares).

edge of the filter. Then we measured the reflectivity of the witness flat at an incident angle of 10° by keeping the sample and the detector fixed. After that, we fixed the incident angle to 10° and let the detector scan the diffraction angular spectrums of the multilayer grating at wavelengths in increments of 0.12 nm from 12.47 to 16.79 nm .

Figure 2 shows the measured reflectivity of the aperiodic multilayer coating and the measured -2nd -order diffraction efficiency of the multilayer grating. In the design wavelength region of $13\text{--}16\text{ nm}$, the aperiodic multilayer coating has an average reflectivity value of 15.92% . Broad passband of the coating leads to a wide usable spectral region of the multilayer grating. The average diffraction efficiency is 9.83% in the region of $13\text{--}16\text{ nm}$.

For comparison, we illustrate the measured reflectivity of a periodic multilayer coating and the measured diffraction efficiency of the periodic multilayer-coated blazed grating in Fig. 2. The 40 bilayer Mo/Si coating has a periodic thickness of $d = 7.1\text{ nm}$ and a gamma ratio of 0.4 ($\Gamma = d_{\text{Mo}}/d$, where d_{Mo} is the thickness of Mo). The blaze angle of the grating substrate was 1.9° . Although the reflectivity of the periodic multilayer coating has a peak value of $\sim 60\%$, its FWHM bandwidth is only $\sim 0.6\text{ nm}$. As a result, the FWHM bandwidth of the diffraction efficiency is also restricted to $\sim 0.6\text{ nm}$. If we evaluate the useable spectral region by the diffraction efficiency of $\sim 10\%$, the useable spectral region of the periodic multilayer grating is $\sim 0.8\text{ nm}$.

The aperiodic multilayer grating has a usable spectral region of $\sim 3\text{ nm}$, much wider than that of the periodic multilayer grating ($< 1\text{ nm}$). This is because the aperiodic multilayer coating has a broad passband, which is favorable for matching with the broad

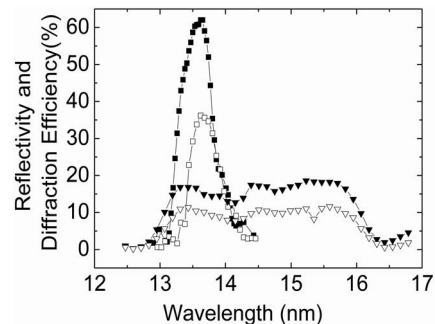


Fig. 2. Measured reflectivity (filled triangles) of the aperiodic multilayer coating and measured -2nd -order diffraction efficiency (empty triangles) of the aperiodic multilayer grating at an incidence angle of 10° , measured reflectivity (filled squares) of the periodic multilayer coating and measured -2nd -order diffraction efficiency (empty squares) of the periodic multilayer grating at an incidence angle of 10° .

bandwidth of the grating groove efficiency. Although the peak diffraction efficiency is inevitably decreased compared with the periodic multilayer grating, the aperiodic multilayer grating had a diffraction efficiency of $\sim 10\%$ through the broad wavelength region, which provides sufficient spectral sensitivity.

There are some differences between the measured reflectivity curve in Fig. 2 and the designed one in Fig. 1. This is due to the difference between the actually produced coating structure and the designed coating structure, which is caused by the existence of interdiffusion regions [10,16,17] and deposition rate errors [10]. Taking the two factors into account, we fit the reflectivity curve to extract the actual coating structure. The best fitted results in Fig. 3 show that (1) interdiffusion regions are asymmetric with Mo-on-Si of 1 nm and Si-on-Mo of 0.6 nm, which are consistent with [16,17], and (2) each Mo layer thickness is 6% smaller than its design value, while the thickness of each Si layer is 6% larger. This actual coating structure was used to calculate the diffraction efficiency of the aperiodic multilayer grating. The calculated efficiency is in good agreement with the measured one, as also shown in Fig. 3.

In conclusion, we have applied an aperiodic multilayer coating on a blazed grating substrate. The coating has a wide passband of 13–16 nm, at which the multilayer grating has an average diffraction efficiency of 9.83% in the -2 nd order. Comparing stan-

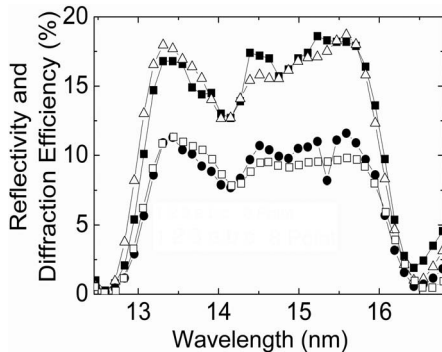


Fig. 3. Measured (filled squares) and calculated (empty triangles) reflectivity of the aperiodic multilayer coating using the actual coating structure, measured (filled circles) and calculated (empty squares) -2 nd-order diffraction efficiencies of the aperiodic multilayer grating at an incidence angle of 10° with the actual coating structure and the blaze and antiblaze angles deduced from AFM results.

dard multilayer gratings with periodic multilayer coatings, this new kind of multilayer grating has a broader usable spectral region. The broadening of the usable spectral region is due to the broadband characteristic of the aperiodic multilayer coating. Combining advantages of the broad usable spectral region and high diffraction efficiency, the aperiodic multilayer grating could be used in EUV spectrograph applications with broadband requirements.

We are grateful to Shu Pei of the State Key Laboratory of Applied Optics of China for AFM measurements. This work is supported by an internal fund of the State Key Laboratory and by the National Natural Science Foundation of China (NSFC) under project 60678034.

References

1. M. P. Kowalski, R. G. Cruddace, J. F. Seely, J. C. Rife, K. F. Heidemann, U. Kleineberg, K. Osterried, D. Menke, and W. R. Hunter, *Opt. Lett.* **22**, 834 (1997).
2. H. Lin, L. Zhang, C. Jin, H. Zhou, and T. Huo, "Fabrication and efficiency measurement of a multilayer-coated ion-beam-etched laminar grating for the extreme-ultraviolet region," *Chin. Opt. Lett.* (to be published).
3. M. P. Kowalski, R. G. Cruddace, T. W. Barbee, Jr., W. R. Hunter, K. F. Heidemann, B. Nelles, R. Lenke, and H. Kierey, *Proc. SPIE* **5488**, 910 (2004).
4. H. Lin, L. Zhang, L. Li, C. Jin, H. Zhou, and T. Huo, *Opt. Lett.* **33**, 485 (2008).
5. B. Vidal, P. Vincent, P. Dhez, and M. Nevière, *Proc. SPIE* **563**, 142 (1985).
6. J. F. Seely, *Proc. SPIE* **4138**, 174 (2000).
7. I. V. Kozhevnikov, I. N. Bukreeva, and E. Ziegler, *Nucl. Instrum. Methods Phys. Res. A* **460**, 424 (2001).
8. S. Yulin, T. Kuhlmann, T. Feigl, and N. Kaiser, *Proc. SPIE* **5037**, 286 (2003).
9. Z. Wang and A. G. Michette, *J. Opt. A* **2**, 452 (2000).
10. A. Aquila, F. Salmassi, F. Dollar, Y. Liu, and E. M. Gullikson, *Opt. Express* **14**, 10073 (2006).
11. R. Souffi and E. M. Gullikson, *Appl. Opt.* **37**, 1713 (1998).
12. R. Souffi and E. M. Gullikson, *Appl. Opt.* **36**, 5499 (1997).
13. H. Lin and L. Li, *Appl. Opt.* **47**, 6212 (2008).
14. M. P. Kowalski, W. R. Hunter, and T. W. Barbee, Jr., *Appl. Opt.* **45**, 305 (2006).
15. M. Nevière, *J. Opt. Soc. Am. A* **8**, 1468 (1991).
16. D. G. Stearns, M. B. Stearns, Y. Cheng, J. Stith, and N. M. Ceglio, *J. Appl. Phys.* **67**, 2415 (1990).
17. S. Bajt, D. G. Stearns, and P. Kearney, *J. Appl. Phys.* **90**, 1017 (2001).